Received January 1999
Revised June 1999
Accepted August 1999

The Stokes problem for a dusty fluid in the presence of magnetic field, heat generation and wall suction effects

Ali J. Chamkha
Department of Mechanical and Industrial Engineering, Kuwait University, Safat, Kuwait

Keywords *Buoyancy, Magnetic fields, Finite differences, Fluids*

Abstract *This work focuses on the laminar flow of a two-phase particulate suspension induced by a suddenly accelerated infinite vertical permeable surface in the presence of fluid buoyancy, magnetic field, heat generation or absorption, and surface suction or blowing effects. The governing equations for this modified Stokes problem are developed based on the continuum representation of both the fluid and the particle cloud. Appropriate dimensionless variables are introduced. The resulting dimensionless equations are solved numerically by an accurate implicit finite-difference method for two situations. The first case corresponds to an impulsive start of the surface from rest while the second case corresponds to a uniformly accelerated surface. The numerical results for these cases are illustrated graphically. Comparisons with previously published work are performed and the results are found to be in good agreement. Typical fluid- and particle-phase velocity and temperature distributions as well as wall shear stress and heat transfer results are reported for various values of the particle loading, Hartmann number, wall mass transfer coefficient and the heat generation or absorption coefficient.*

Nomenclature

B_0 = Magnetic field strength
c = Fluid-phase specific heat at constant pressure
C = Fluid-phase skin-friction coefficient ($C = -\partial F/\partial\eta(\tau,0)$)
F = Dimensionless fluid-phase tangential velocity ($F = u/v_0$)
g = Acceleration due to gravity
G = Numerical growth factor
Gr = Grashof number ($Gr = g\beta^*\nu(T_w - T_\infty)/U_0^3$)
Ha = Hartmann number ($Ha = B_0/U_0(\sigma\nu/\rho)^{1/2}$)
k = Stokes drag coefficient ($k = 6\pi\mu r$)
K = Fluid-phase thermal conductivity
m = Particle mass
n = Wall velocity exponent
N_0 = Particle number density
p = Fluid-phase pressure
Pr = Fluid-phase Prandtl number ($Pr = \mu c/K$)
q_w = Wall heat transfer coefficient
Q_0 = Dimensional heat generation or absorption coefficient
r = Particle radius
r_v = Dimensionless wall mass transfer ($r_v = v_0/U_0$)
t = Time
T = Dimensional fluid-phase temperature
u = Dimensional x-component (vertical) of velocity
U_0 = Surface velocity
v = Dimensional y-component (horizontal) of velocity
v_0 = Wall suction or injection velocity
x, y = Cartesian coordinates

Greek symbols

α = Inverse Stokes number ($\alpha = \nu/(\tau_p U_0^2)$)
β^* = Thermal expansion coefficient
η = Dimensionless normal distance
ϕ = Dimensionless heat generation or absorption coefficient ($\phi = Q_0\nu/(\rho c U_0^2)$)

International Journal of Numerical Methods for Heat & Fluid Flow, Vol. 10 No. 1, 2000, pp. 116-133.

γ = Ratio of specific heats ($\gamma = c_p/c$)
κ = Particle loading ($\kappa = N_0 m/\rho$)
μ = Fluid-phase dynamic viscosity
ν = Fluid-phase kinematic viscosity
ρ = Fluid-phase density
σ = Fluid-phase electrical conductivity
τ = Dimensionless time ($\tau = v_0 t/\nu$)
τ_p = Velocity relaxation time
τ_T = Thermal equilibrium time ($\tau_T = 3c_p \tau_p Pr/(2c)$)
θ = Dimensionless fluid-phase temperature ($\theta=(T-T_\infty)/(T_w - T_\infty)$)

Subscripts
p = Particle phase
w = Wall
∞ = Free stream

Introduction

This paper considers laminar flow of a viscous dusty fluid past an impulsively moving infinite vertical surface or plate in the presence of fluid buoyancy effects and a magnetic field applied in the horizontal direction normal to the flow. The plate is assumed to be permeable so as to allow for possible wall suction or injection and is considered to be electrically non-conducting. The fluid phase is assumed to be incompressible, Newtonian, viscous, electrically conducting and heat generating or absorbing. The particle phase is assumed to be made up of spherical particles having uniform size and density distribution and is considered as an electrical insulator. This flow and heat transfer situation arises in many engineering, manufacturing and metallurgical applications such as glass blowing, extrusion processes, continuous casting, cooling of metallic sheets, cooling of electronic chips, crystal growing, melt spinning and many others.

The flow of an incompressible fluid over an impulsively-started horizontal surface which is often referred to as the Stokes or Rayleigh flow problem was initially analyzed some time ago by Stokes (1951). Since then, different versions of the problem with various physical effects have been investigated by different authors. Among these are Stewartson (1951), Hall (1969) and Elliott (1969). Soundalgekar (1977) has reported on the effects of free convection currents on the single-phase Stokes problem when the vertical plate is impulsively started from rest. Foote *et al.* (1987) have reported some exact solutions for the Stokes problem for an elastico-viscous fluid using the Taylor series expansion which compared with the perturbation solutions obtained in some earlier investigations. Other related work are those of Wang (1984), who considered liquid film flow on an unsteady stretching surface, Smith (1994), who reported an exact solution of the unsteady Navier-Stokes equations resulting from a stretching surface, and Chamkha (1999), who studied the effects of magnetic field and heat generation or absorption on the unsteady flow of a continuously stretching semi-infinite surface. Although the flow of a two-phase particulate suspension over an infinite horizontal permeable fixed plate has been considered extensively in the literature (see Apazidis, 1985, 1990; Chamkha and Peddieson, 1990), little work has been reported on the problem of two-phase flow over an impulsively-started surface. Apazidis (1985) has considered, among other things, laminar flow of a particulate suspension in the presence of a gravity field caused by a suddenly accelerated surface. Recently,

Ramamurthy (1987, 1990) has discussed the problem of free convection effects on the Stokes flow and heat transfer for an infinite vertical plate in a dusty fluid. Ramamurthy (1990) has considered two situations (when the plate is started impulsively from rest and when the plate is uniformly accelerated) and his solutions were obtained by the Laplace transform technique. It is of interest in the present work to generalize the work of Ramamurthy (1990) to include wall suction or injection effects and hydromagnetic and fluid heat generation or absorption effects.

Problem formulation

Consider laminar incompressible flow of an electrically-conducting and heat-generating or absorbing dusty fluid over a vertical permeable impulsively-started infinite surface in the presence of a uniformly applied magnetic field. The surface is maintained at a constant temperature and occupies the plane $x = 0$ and the flow of the dusty fluid is in the xy plane. Far from the surface, both the fluid and the dust particles are in equilibrium and are assumed to be at rest. The dust or particle-phase volume fraction is assumed to be small and the suspension is assumed to be dilute in the sense that interparticle collision is neglected.

Also, all particles are assumed to be spheres of uniform size and density. The magnetic Reynolds number is assumed to be small so that the induced magnetic field is neglected. While the fluid phase is assumed to be electrically conducting, both the particle phase and the surface are assumed to be electrically non-conducting. In addition, all fluid and particle properties are assumed to be constant except the fluid density in the body force term of the fluid-phase momentum equation. By neglecting such effects as the viscous and Joule dissipations, Hall effect, and the drag work and using the Boussinesq approximation, the governing equations for this problem can be written as:

$$\frac{\partial \mathrm{v}}{\partial \mathrm{y}} = 0 \tag{1}$$

$$\rho\left(\frac{\partial \mathrm{u}}{\partial \mathrm{t}} + \mathrm{v}\frac{\partial \mathrm{u}}{\partial \mathrm{y}}\right) = \mu\frac{\partial^2 \mathrm{u}}{\partial \mathrm{y}^2} - \frac{\partial \mathrm{p}}{\partial \mathrm{x}} + \mathrm{kN}_0(\mathrm{u}_\mathrm{p} - \mathrm{u}) - \sigma \mathrm{B}_0^2 \mathrm{u} - \rho \mathrm{g} \tag{2}$$

$$\rho \mathrm{c}\left(\frac{\partial \mathrm{T}}{\partial \mathrm{t}} + \mathrm{v}\frac{\partial \mathrm{T}}{\partial \mathrm{y}}\right) = \mathrm{K}\frac{\partial^2 \mathrm{T}}{\partial \mathrm{y}^2} + \frac{\mathrm{N}_0 \mathrm{mc}_\mathrm{p}}{\tau_\mathrm{T}}(\mathrm{T}_\mathrm{p} - \mathrm{T}) + \mathrm{Q}_0(\mathrm{T} - \mathrm{T}_\infty) \tag{3}$$

$$\frac{\partial \mathrm{v}_\mathrm{p}}{\partial \mathrm{y}} = 0 \tag{4}$$

$$\rho_\mathrm{p} \mathrm{c}_\mathrm{p}\left(\frac{\partial \mathrm{u}_\mathrm{p}}{\partial \mathrm{t}} + \mathrm{v}_\mathrm{p}\frac{\partial \mathrm{u}_\mathrm{p}}{\partial \mathrm{y}}\right) = -\rho_\mathrm{p}\frac{(\mathrm{u}_\mathrm{p} - \mathrm{u})}{\tau_\mathrm{p}} \tag{5}$$

$$\rho_p c_p \left(\frac{\partial T_p}{\partial t} + v_p \frac{\partial T_p}{\partial y} \right) = \frac{\rho_p c_p (T_p - T)}{\tau_T} \tag{6}$$

where t stands for time and x and y denote the tangential (vertical) and normal (horizontal) distances, respectively. u, v, p and T are the fluid-phase x-component (vertical) of velocity, y-component (horizontal) of velocity, pressure, and temperature, respectively. ρ, μ, c, K and σ are the fluid-phase density, dynamic viscosity, coefficient of specific heat, thermal conductivity and the electrical conductivity, respectively. B_0, g, and Q_0 are the applied magnetic induction, acceleration due to gravity, and the dimensional heat generation (> 0) or absorption (< 0) coefficient, respectively. k, N_0, m, τp, τT and T_∞ are the Stokes drag coefficient (= 6πμr for spherical particles of radius r), particle number density, particle mass, velocity relaxation (or equilibrium) time (= m/k), thermal equilibrium time($= \frac{3}{2}\frac{c_p}{c} Pr \tau_p$, $Pr = \mu c/K$ is the Prandtl number) and the free stream temperature, respectively. The subscript p stands for the particle phase.

The initial and boundary conditions for this problem can be written as:

$$u(0,y) = u_p(0,y) = 0, \; T(0,y) = T_p(0,y) = T_\infty \tag{7}$$

$$u(t,0) = \frac{{U_0}^{2n+1}}{\nu^n} t^n, \; v(t,0) = -v_0, \; v_p(t,0) = -v_0, \; T(t,0) = T_w$$

$$u(t,\infty) = 0, T(t,\infty) = T_\infty, \; T_p(t,\infty) = T_\infty, t > 0 \tag{8a-g}$$

where U_0, ν and "n" are the surface velocity, fluid-phase kinematic viscosity (μ/ρ) and the wall velocity exponent, respectively. v_0 and T_w are the suction velocity and the wall temperature, respectively.

Equations (1) and (4) subject to Equations (8c) and (8d) are satisfied by

$$v = v_p = -v_0 \tag{9}$$

Using this, evaluating Equation (2) at the free stream with $u_p(t,\infty) = 0$, invoking the Boussinesq approximation and rearranging yield

$$\frac{\partial u}{\partial t} - v_0 \frac{\partial u}{\partial y} = \nu \frac{\partial^2 u}{\partial y^2} + \beta^* g (T - T_\infty) + \frac{k N_0}{\rho} (u_p - u) - \frac{\sigma B_0^2}{\rho} u \tag{10}$$

where β* is the thermal expansion coefficient.

Following Ramamurthy (1990), it is convenient to employ the following dimensionless variables:

$$\tau = \frac{v_0^2 t}{\nu}, \eta = \frac{v_0 y}{\nu}, F = \frac{u}{v_0}, F_p = \frac{u_p}{v_0}, \theta = \frac{T - T_\infty}{T_w - T_\infty}, \theta_p \frac{T_p - T_\infty}{T_w - T_\infty} \tag{11}$$

in Equations (10), (5), (3), and (6) to respectively give:

$$\frac{\partial F}{\partial \tau} - r_v \frac{\partial F}{\partial \eta} = \frac{\partial^2 F}{\partial \eta^2} + \kappa\alpha(F_p - F) - Ha^2 F + Gr\theta \tag{12}$$

$$\frac{\partial F_p}{\partial \tau} - r_v \frac{\partial F_p}{\partial \tau} = -\alpha(F_p - F) \tag{13}$$

$$\frac{\partial \theta}{\partial \tau} - r_v \frac{\partial \theta}{\partial \eta} = \frac{1}{Pr}\frac{\partial^2 \theta}{\partial \eta^2} - \frac{2}{3}\frac{\kappa\alpha}{Pr}(\theta_p - \theta) + \phi\theta \tag{14}$$

$$\frac{\partial \theta_p}{\partial \tau} - r_v \frac{\partial \theta_p}{\partial \eta} = -\frac{2}{3}\frac{\alpha}{Pr\gamma}(\theta_p - \theta) \tag{15}$$

where

$$r_v = \frac{v_0}{U_0}, Gr = \frac{g\beta^* \nu (T_w - T_\infty)}{U_0^3}, \kappa = \frac{N_0 m}{\rho}, \alpha = \frac{\nu}{\tau_p U_0^2}$$

$$Ha^2 = \frac{\sigma B_0^2 \nu}{\rho U_0^2}, \phi = \frac{Q_0 \nu}{\rho c U_0^2}, \gamma = \frac{c_p}{c} \tag{16}$$

are the dimensionless wall mass transfer coefficient, Grashof number, particle loading, inverse Stokes number, square of the Hartmann number, dimensionless heat generation or absorption coefficient and the ratio of specific heats, respectively.

The dimensionless initial and boundary conditions become:

$$F(0,\eta) = 0, F_p(0,\eta) = 0, \theta(0,\eta) = 0, \theta_p(0,\eta) = 0 \tag{17}$$

$$F(\tau,0) = \tau^n, \theta(\tau,0) = 1$$

$$F(\tau,\infty) = 0, F_p(\tau,\infty) = 0, \theta(\tau,\infty) = 0, \theta_p(\tau,\infty) = 0 \qquad (18a-f)$$

Important physical parameters for this flow and heat transfer situation are the fluid-phase skin-friction coefficient C, and the wall heat transfer coefficient q_w. These are defined, respectively as:

$$C = \frac{\tau^*(t,0)}{\rho U_0^2} = -\frac{\partial F}{\partial \eta}(\tau,0), \ \tau^* = -\mu\frac{\partial u}{\partial y}(t,0) \tag{19}$$

$$q_w = \frac{q_w^*}{KU_0(T_w - T_\infty)/\nu} = -\frac{\partial \theta}{\partial \eta}(\tau,0), \ q_w^* = -K\frac{\partial T}{\partial y}(t,0) \tag{20}$$

Results and discussion

Since the solution of the governing equations by the Laplace transform or any other analytical method is too involved and requires difficult numerical evaluations, Equations (12) through (15) were solved subject to the initial and boundary conditions given by Equation (17) by the implicit tridiagonal finite-difference method discussed by Blottner (1970). All first-order derivatives with respect to τ are first replaced by two-point backward-difference formulae. Then, three-point central difference quotients are used to discretize all second-order differential equations in η while all first-order differential equations in η are discretized using the trapezoidal rule. With this, the governing equations are converted into a set of linear algebraic equations which are then solved by the well-known Thomas algorithm. The problem is solved line by line at different τ locations. Constant step sizes of 0.01 are used in the τ direction while variable step sizes in the η direction are employed to accommodate the rapid changes of the variable in the immediate vicinity of the wall. The initial step size and growth factor used were $\Delta\eta_1 = 0.001$ and G = 1.03 such that $\Delta\eta_{n+1} = G\Delta\eta_n$. These values were arrived at after many numerical experiments performed to assess grid-size independence.

The convergence criterion employed was based on the relative difference between the current and the previous iterations. When this difference reached 10^{-6}, the solution was assumed converged and the iteration process was terminated. A representative set of numerical results is displayed graphically in Figures 1-18.

In order to validate the accuracy of the numerical results to be reported subsequently, comparisons of the fluid-phase skin-friction coefficient and the wall heat transfer with those reported previously by Ramamurthy (1990) are performed and the results are given in Tables I and II. It is seen from these Tables that good agreements between the results exist. The small deviations of the results of Ramamurthy (1990) in some cases are probably due to the numerical evaluation of the non-standard functions obtained by his analysis using the Laplace transform method.

Figures 1-4 present time histories for the profiles of the fluid-phase velocity F, particle-phase velocity F_p, the fluid-phase temperature θ, and the particle-phase temperature θ_p, respectively for both conditions of impulsive start of the surface from rest (n = 0) and uniformly accelerated surface (n = 1). It is seen from the Figures that the development of the hydrodynamic layers is faster than the thermal layers of both phases. Also, it is seen that the velocity and temperature profiles of both phases increase with time for both conditions of impulsive surface start from rest (n = 0) and uniformly accelerated surface (n = 1) and that the velocities are lower for n = 1 than for n = 0. The temperature profiles of both phases are unaffected by changes in the values of n since the temperature fields are uncoupled from the velocity fields, as is obvious from Equations (14) and (15).

Figures 5-8 illustrate the effects of the particle loading κ on the velocity profiles of the fluid and particle phases F and F_p and the temperature profiles

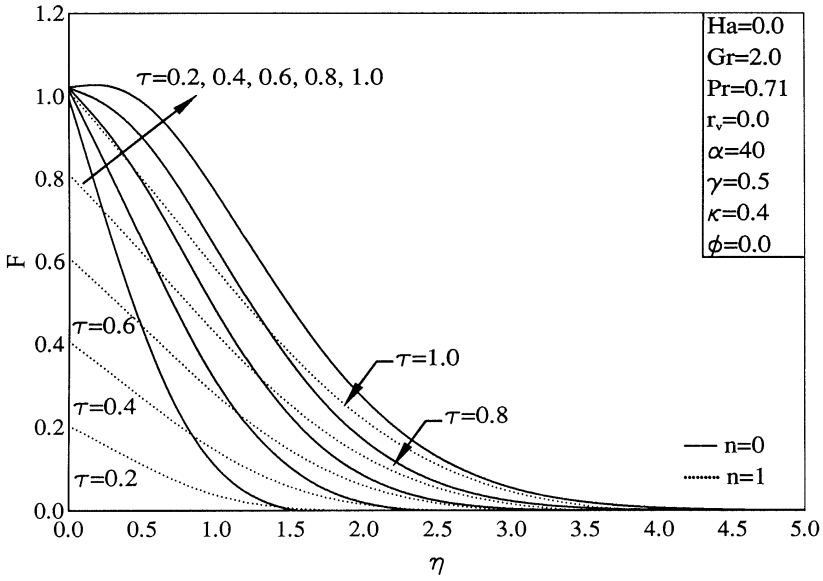

Figure 1.
Time history for fluid-phase velocity profiles

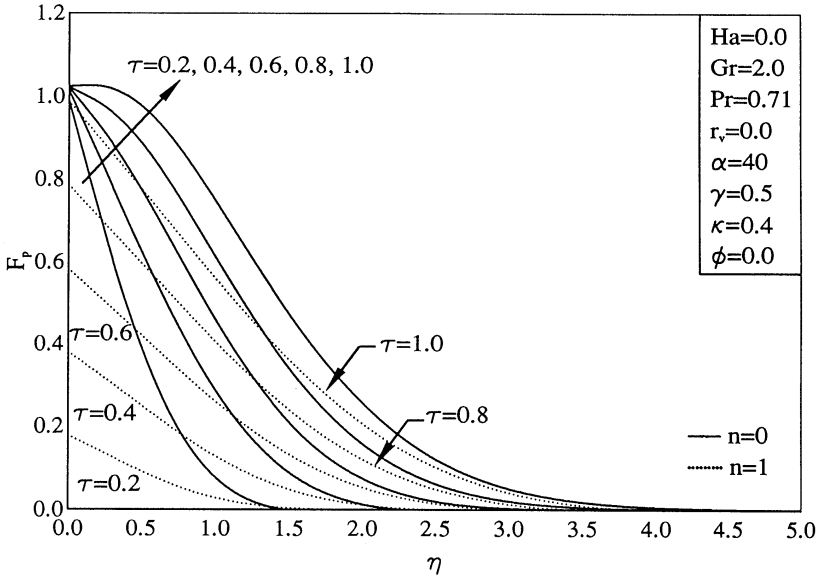

Figure 2.
Time history for particle-phase velocity profiles

for the fluid and particle phases θ and θ_p for the condition of n = 0 and n = 1, respectively. Increases in the particle loading have the tendency to increase the drag force and the heat exchange between the phases. This results in reductions in the flow velocities and temperatures of both phases for aiding flow (Gr > 0), as is evident in Figures 5-8, and increases in these velocities

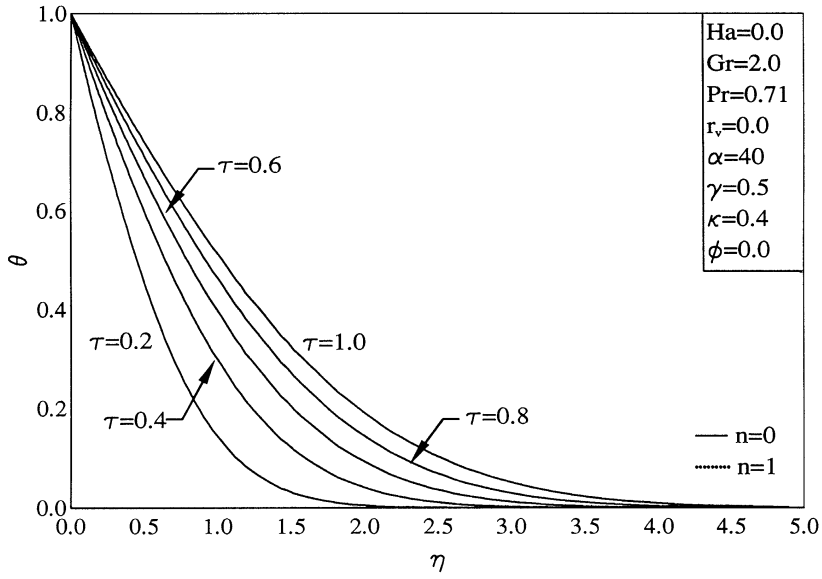

Figure 3.
Time history for fluid-phase temperature

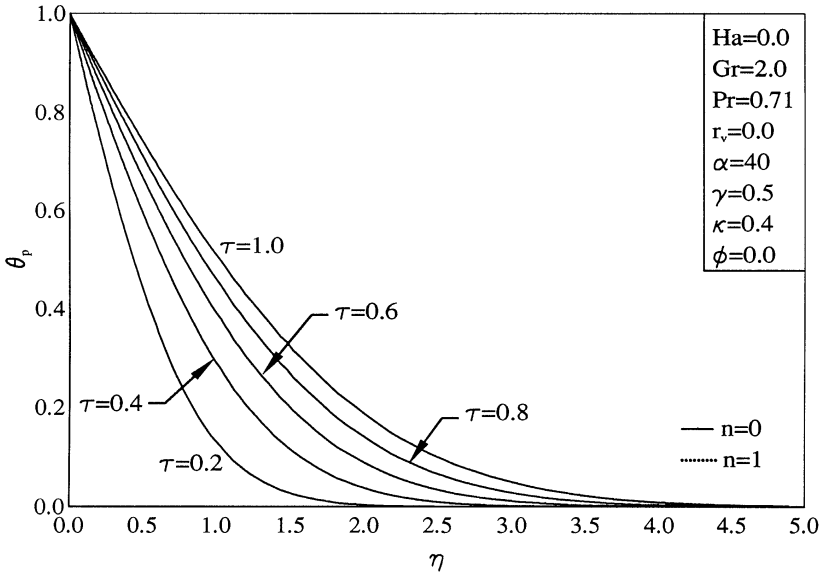

Figure 4.
Time history for particle-phase temperature profiles

for opposing flows (Gr < 0). The reduction in the fluid-phase temperature as a result of increasing k produces enhancements in the wall heat transfer.

The influence of the Hartmann number Ha on the velocity profiles F and F_p is shown in Figures 9 and 10, respectively. Application of a magnetic field normal to the flow direction gives rise to a drag-like force in the direction

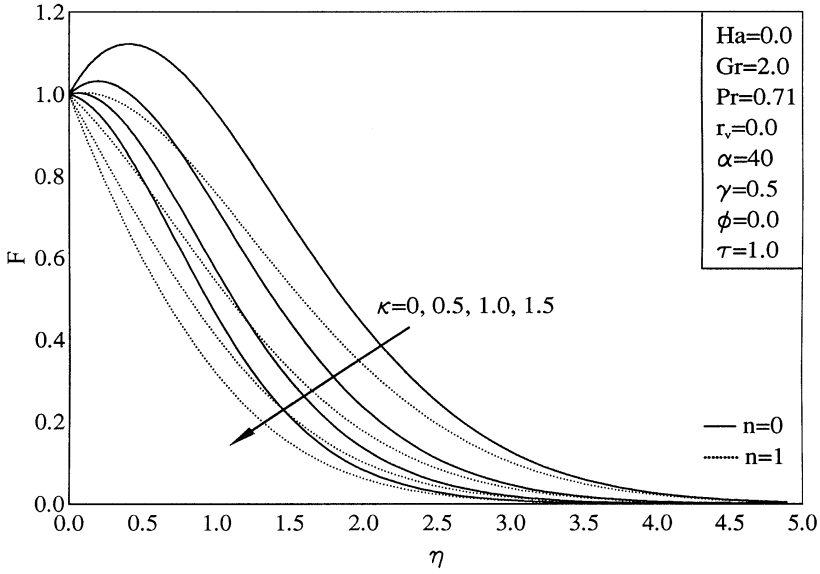

Figure 5.
Effects of κ on fluid-phase velocity profiles

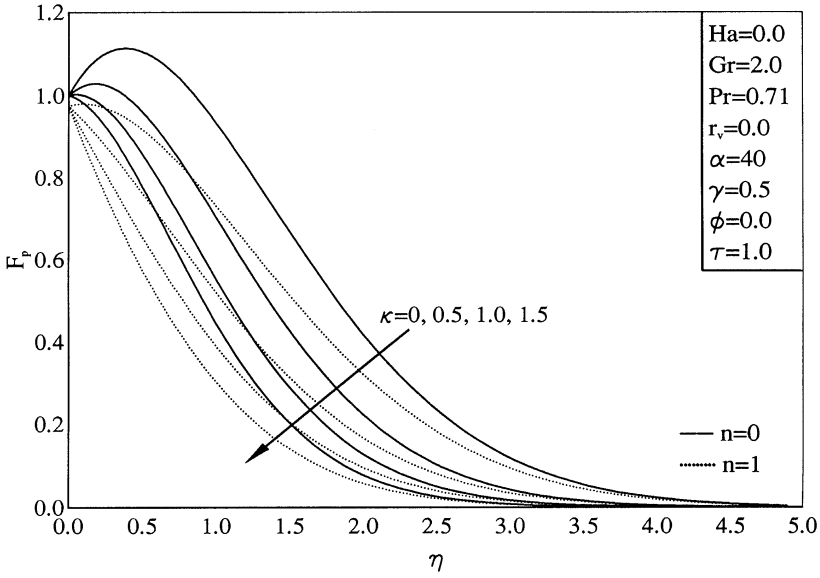

Figure 6.
Effects of κ on particle-phase velocity profiles

opposite to the flow. This force is called the Lorentz force. This resistive force causes the flow of the fluid phase and, in turn, the particle phase (through the drag force) along the surface to decrease. This is represented by the decreases of F and F_p as Ha increases, shown in Figures 9 and 10. It is also evident from these Figures that while the differences in the velocities of both phases for n = 0 and n = 1 are significant for Ha = 0, they tend to vanish for large values of Ha (Ha = 4).

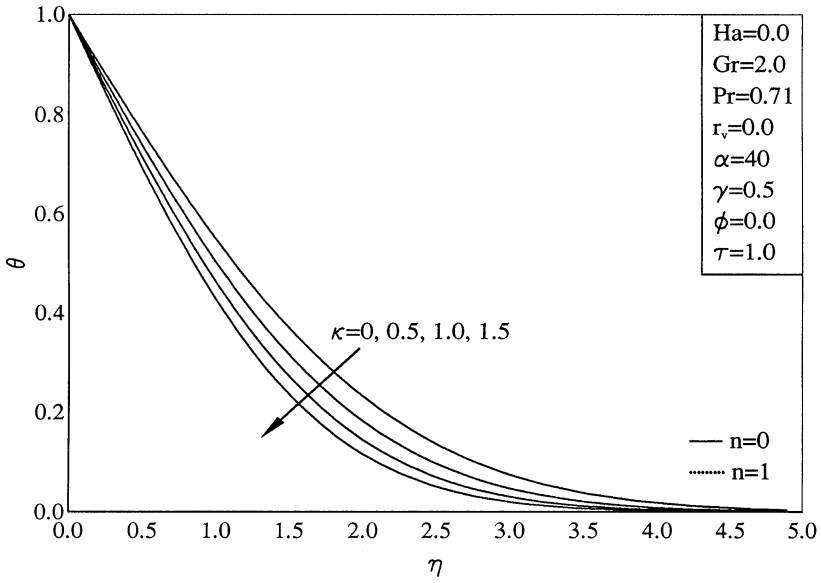

Figure 7.
Effects of κ on fluid-phase temperture profiles

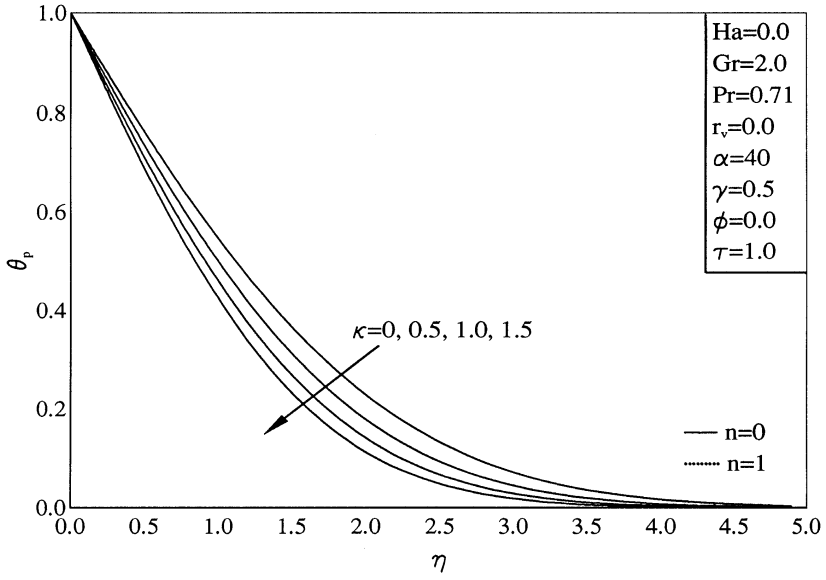

Figure 8.
Effects of κ on particle-phase temperature profiles

Figures 11-14 depict the influence of the wall mass transfer coefficient r_v on the profiles of F, F_p, θ, and θ_p, respectively. Imposition of fluid-phase (and particle-phase) wall suction ($r_v > 0$) causes both the velocity and temperature layers of both phases to decrease. Also, the velocity and temperature distributions of both phases reduce at every point far from the surface. Conversely, fluid-phase (and particle-phase) injection ($r_v < 0$) at the wall produces the opposite effect,

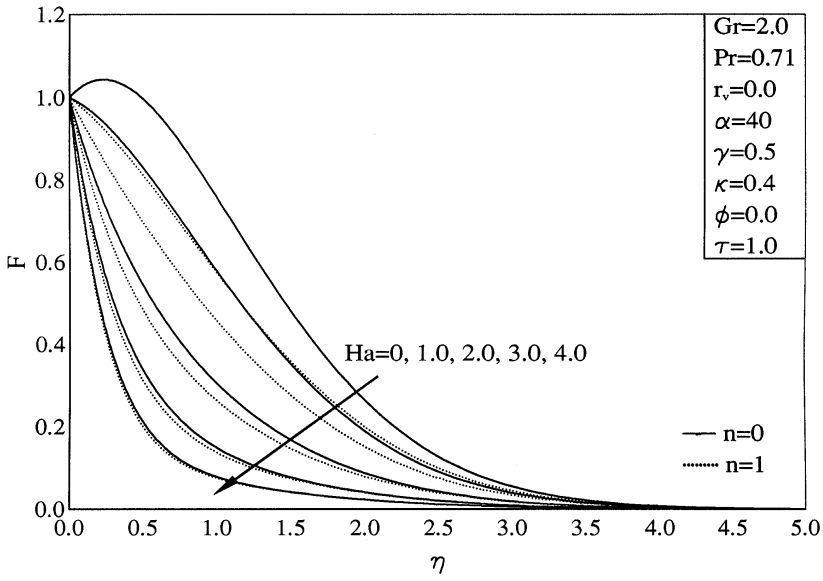

Figure 9.
Effects of Ha on fluid-phase velocity profiles

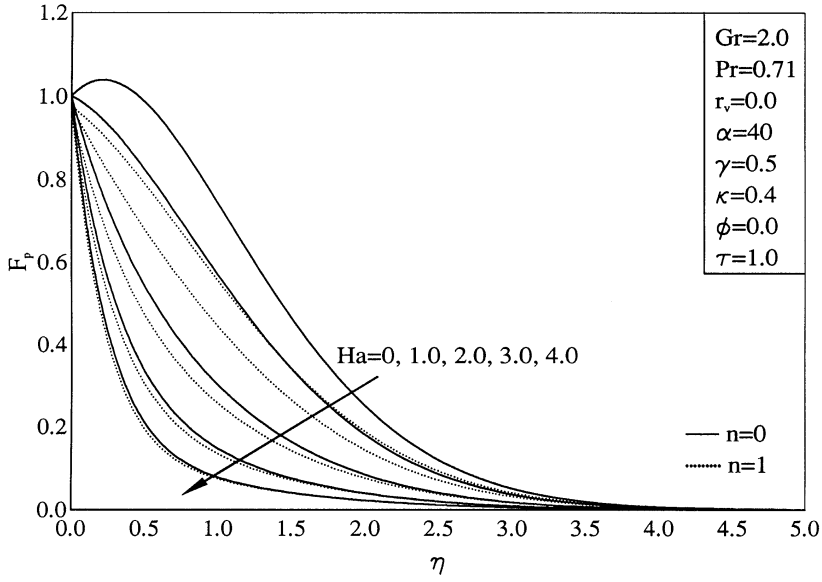

Figure 10.
Effects of Ha on particle-phase velocity profiles

namely an increase in the velocity and temperature distributions as well as in the hydrodynamic and thermal layers of both phases. Figures 11 and 12 also show that for $r_v < 0$ distinctive peaks appear in the fluid- and particle-phase velocity profiles close to the surface and that these peaks tend to shift further from the surface as r_v decreases. These and the previous facts are evident in Figures 11-14.

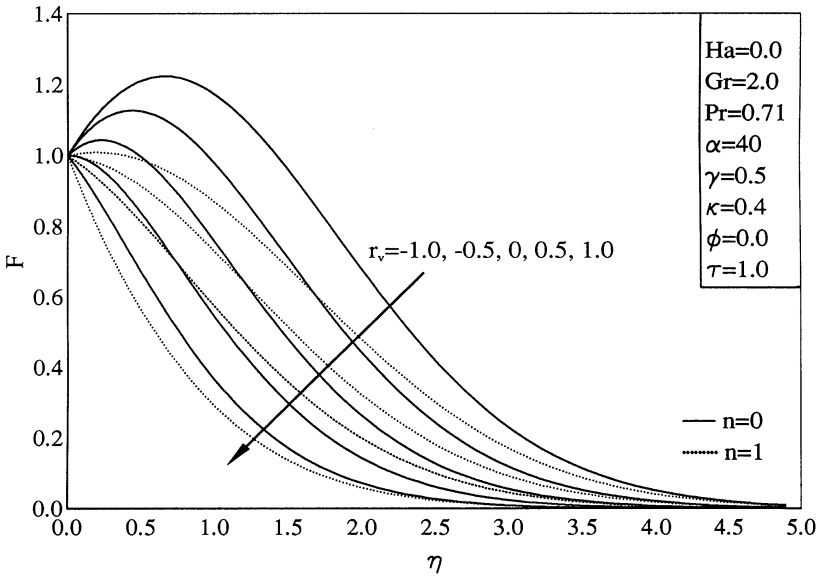

Figure 11.
Effects of r_v on fluid-phase velocity profiles

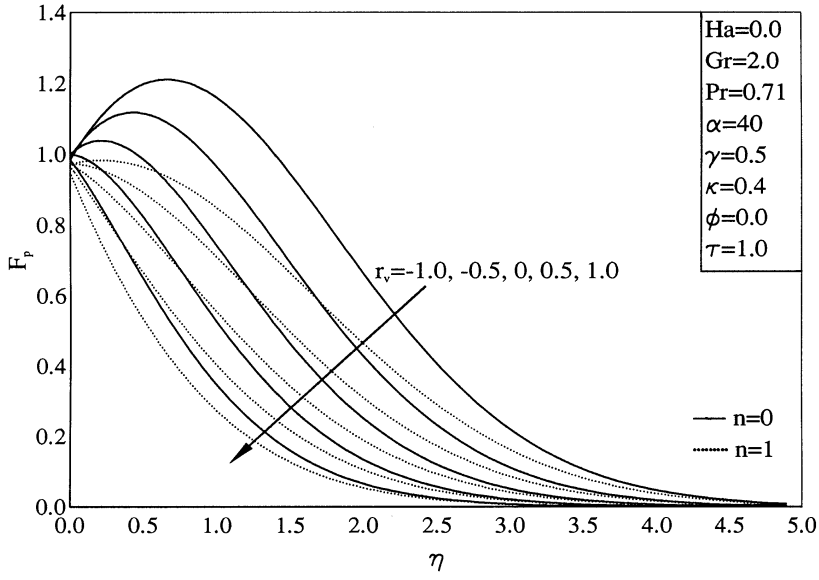

Figure 12.
Effects of r_v on particle-phase velocity profiles

Figures 15-18 display the effects of the fluid-phase heat generation or absorption coefficient ϕ on the profiles of F, F_p, θ, and θ_p, respectively. Heat generation ($\phi > 0$) causes the temperature of the fluid to increase. Consequently, and through interphase heat transfer, the particle phase temperature increases. The enhancement in the fluid-phase temperature enhances the thermal buoyancy effect which causes higher induced suspension

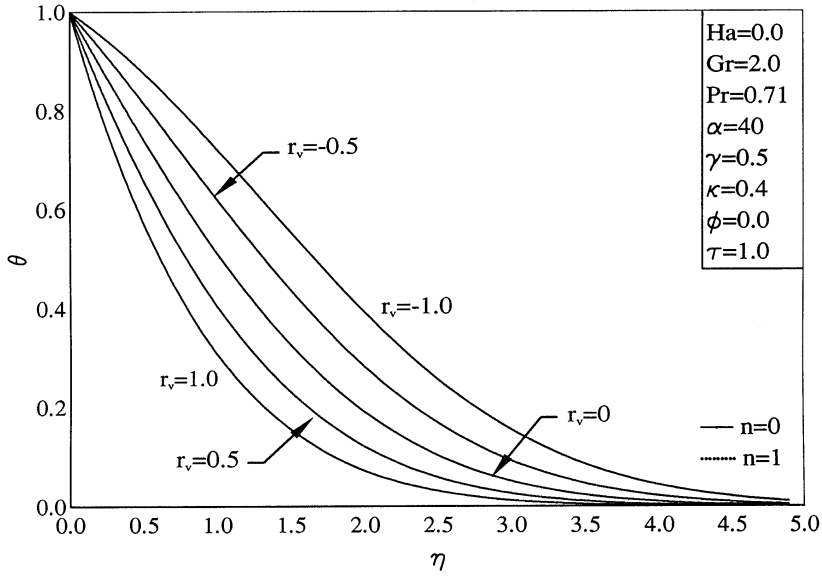

Figure 13.
Effects of r_v on fluid-phase temperature profiles

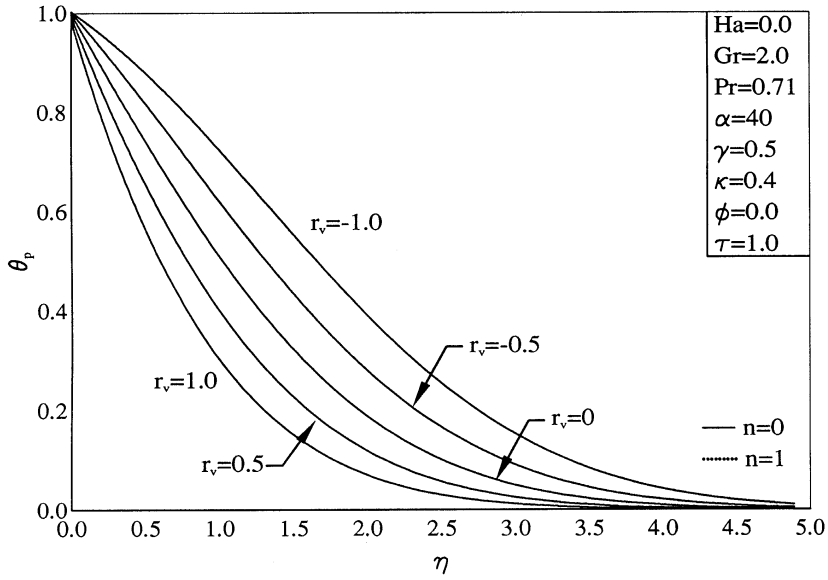

Figure 14.
Effects of r_v on particle-phase temperture profiles

velocities. On the contrary, heat absorption produces the opposite effect represented by decreases in F, F_p, θ, and θ_p. These facts are clearly seen from Figures 15-18.

From other results, not shown here for brevity, it is observed that increasing the Grashof number Gr produces the same effect as increasing ϕ as they both increase the thermal buoyancy effect. However, increasing the inverse Stokes

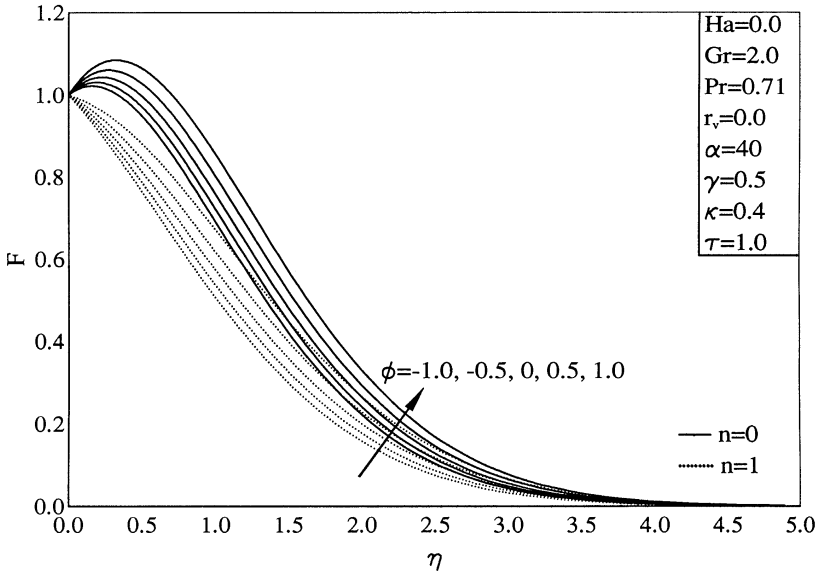

Figure 15.
Effects of ϕ on fluid-phase velocity profiles

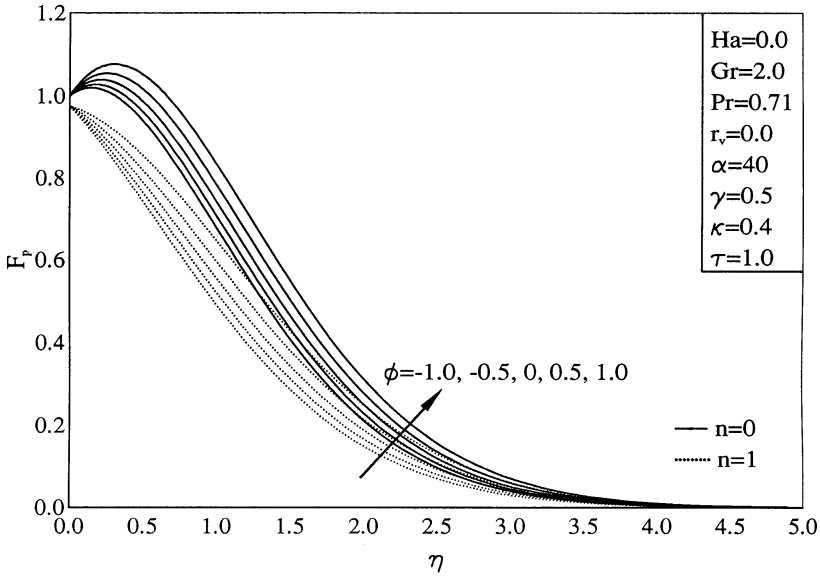

Figure 16.
Effects of ϕ on particle-phase velocity profiles

number a increases the interphase coupling between the phases causing the fluid-phase velocity to decrease and the particle-phase velocity and temperature to increase. These behaviours are also observed from the non-shown results.

Tables III-V depict the influences of r_v, Ha, ϕ, κ and α on the fluid-phase skin friction coefficient C and the wall heat transfer coefficient q_w. It is clearly

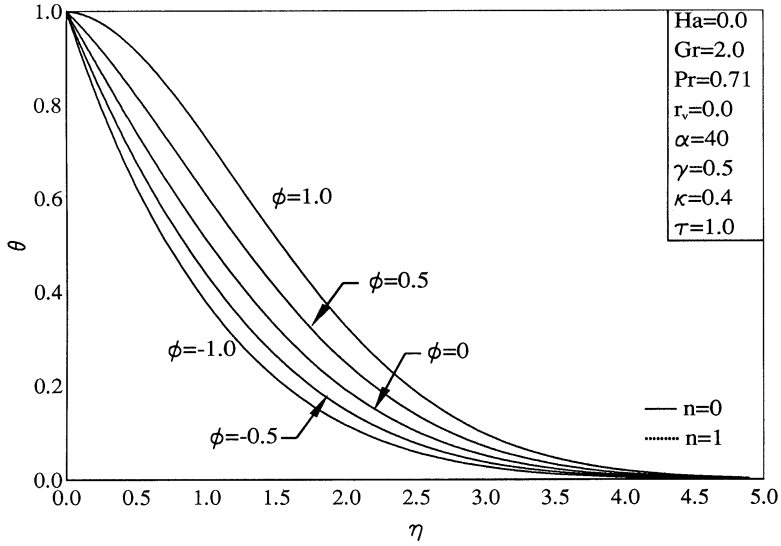

Figure 17.
Effects of ϕ on fluid-phase temperature

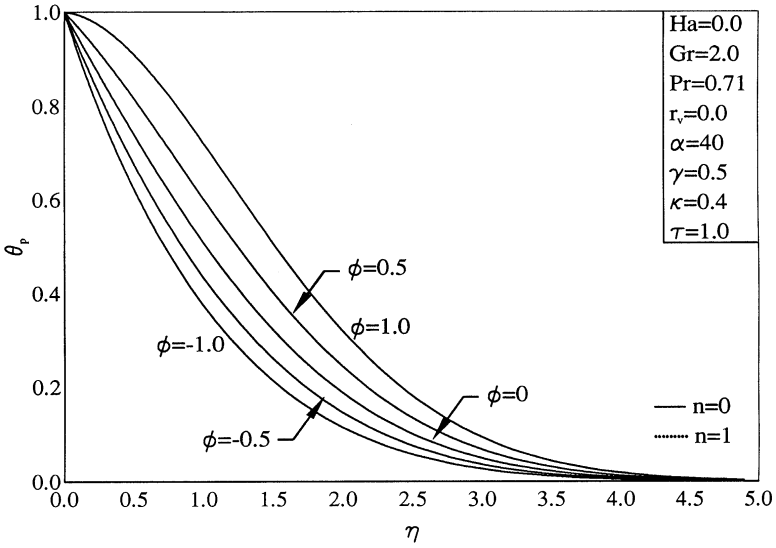

Figure 18.
Effects of ϕ on particle-phase temperature profiles

τ	0.2	0.4	0.6	1.0	2.0
q_w Ramamurthy (1990)	1.11490	0.78830	0.64360	0.49860	0.35350
q_w Present work	1.14013	0.79812	0.64971	0.50223	0.35467
C Ramamurthy (1990)	0.87200	0.25600	–0.08530	–	–
C Present work	0.91186	0.27072	–0.07671	–0.51685	–1.17251

Note: Gr = 2.0, Ha = 0, n = 0, Pr = 0.71, r_v = 0, α = 40, γ = 0.5, κ = 0.2, and ϕ = 0

Table I.
Comparison of q_w and C values with Ramamurthy (1990)

Gr	Pr	κ	Ramamurthy (1990)	Present work
2.0	0.71	0	–0.22030	–0.21264
2.0	0.71	0.4	0.03180	0.04132
–2.0	0.71	0	1.67700	1.68087
–2.0	0.71	0.4	1.69170	1.70114
2.0	7.0	0	0.24890	0.25565
2.0	7.0	0.4	0.43350	0.44025
–2.0	7.0	0	1.20780	1.21280
–2.0	7.0	0.4	1.29010	1.30237

Note: Ha = 0, n = 0, r_v = 0, α = 40, γ = 0.5, ϕ = 0, and τ = 0.6

Table II. Comparison of C values with Ramamurthy (1990)

	r_v = –1.0			r_v = 0			r_v = 1.0		
τ	0.1	0.5	1.0	0.1	0.5	1.0	0.1	0.5	1.0
C	1.18314	–0.31601	–0.76428	1.71051	0.07852	–0.51685	2.33597	0.78262	0.24530
q_w	1.28806	0.38937	0.20602	1.64911	0.71246	0.50223	2.06702	1.16989	0.98636

Note: Gr = 2, Ha = 0, n = 0, Pr = 0.71, α = 40, γ = 0.5, κ = 0.2, and ϕ = 0.

Table III. Values of C and q_w for various r_v and τ values

	ϕ = –1.0			ϕ = 0			ϕ = 1.0		
Ha	0	2	4	0	2	4	0	2	4
C	–0.38495	1.34137	3.59555	–0.51685	1.26849	3.56458	–0.70490	1.16306	3.52014
q_w	0.89652	0.89652	0.89652	0.50223	0.50223	0.50223	–0.03513	–0.03513	–0.03513

Note: Gr = 2, n = 0, Pr = 0.71, r_v = 0, α = 40, γ = 0.5, κ = 0.2, and τ = 0.

Table IV. Values of C and q_w for various Ha and ϕ values

	κ = 0	κ = 0.4		κ = 0.6			κ = 0.8		
α	40	40	100	1	40	100	1	40	100
C	–0.65543	0.39893	–0.39835	–0.35785	–0.29504	–0.29465	–0.27182	–0.20206	–0.20248
q_w	0.47876	0.52420	0.52383	0.56311	0.54590	0.54553	0.58987	0.56680	0.56662

Note: Gr = 2, Ha = 0, n = 0, Pr = 0.71, r_v = 0, γ = 0.5, ϕ = 0, and τ = 1.0.

Table V. Values of C and q_w for various κ and α values

observed from these Tables that the values of both C and q_w increase as r_v increases. Also, while the values of C increase significantly as Ha increases, the values of q_w remain unchanged. This is expected since in the absence of viscous and magnetic dissipations, the energy equations are uncoupled from the momentum equations in which the magnetic Lorentz force exists. In addition, as the heat generation or absorption coefficient ϕ increases, the values of both C and q_w decrease. Yet, the effect of ϕ is more pronounced on q_w than

on C. Furthermore, owing the presence of the particles, both the wall heat transfer and the skin-friction coefficient increase. However, while increasing the inverse Stokes number α produces higher values of C, it results in reductions in the wall heat transfer. Finally, as time progresses both C and q_w tend to decrease.

Conclusion

The problem of laminar and heat transfer of a fluid-particle suspension caused by a suddenly accelerated surface in the presence of buoyancy, magnetic field, heat generation or absorption, and surface mass transfer was solved numerically by the finite-difference methodology. Two conditions were considered. The first was when the surface is impulsively-started from rest and the second was when the surface is uniformly accelerated. The numerical results were validated by favorable comparisons with previously reported solutions. It was found that the presence of the magnetic field caused slowing of the motion of the suspension. Also, imposition of fluid and particle surface suction produced lower velocity and temperature distributions of both phases. The opposite was true when fluid and particles were blown from the surface into the main flow. In this situation, distinctive peaks in the velocity profiles of both phases close to the wall were observed. Heat generation was found to increase the suspension flow due to increases in the thermal buoyancy effects. In addition, owing to the presence of particles in the suspension, the velocity distribution of both phases decreased for buoyancy aiding flow and increased for buoyancy opposing flow. It is hoped the present work will be used as a vehicle for investigating more generalized two-phase flow models.

References

Apazidis, N. (1985), "On two-dimensional laminar flows of a particulate suspension in the presence of gravity field", *Int. J. Multiphase Flow*, Vol. 11 No. 5, pp. 675-98.

Apazidis, N. (1990), "Temperature distribution and heat transfer in a particle-fluid flow past a heated horizontal plate", *Int. J. Multiphase Flow*, Vol. 16 No. 3, pp. 495-513.

Blottner, F.G. (1970), "Finite-difference methods of solution of the boundary-layer equations", *AIAA Journal*, Vol. 8, pp. 193-205.

Chamkha, A.J. (1999), "Hydromagnetic three-dimensional free convection on a vertical stretching surface with heat generation or absorption", *Int. J. Heat Fluid Flow*, Vol. 20, pp. 84-92.

Chamkha, A.J. and Peddieson, J. (1990), "Unsteady dusty-gas flow with suction", *Engineering Science*, Preprint Number 27.

Elliott, L. (1969), "Unsteady laminar flow of a gas near infinite flat plate", in Angew, Z. (Ed.), *Math. Mech.*, Vol. 49, p. 647.

Foote, J.R., Puri, P. and Kythe, P.K. (1987), "Some exact solutions of the Stokes problem for an elastico-viscous fluid", *Acta Mechanica*, Vol. 68, pp. 223-30.

Hall, M.G. (1969), "Boundary layer over an impulsively started flated plate", *Proc. Roy. Soc.*, Vol. 310A, p. 401.

Ramamurthy, V. (1987), "Free convection effects on the Stokes problem for an infinite vertical plate in a dusty fluid", *Ph.D. Thesis I.I.T.*, Kharagpur.

Ramamurthy, V. (1990), "Free convection effects on the Stokes problem for an infinite vertical plate in a dusty fluid", *Jour. Math. Phy. Sci.*, Vol. 24 No. 5, pp. 297-312.

Smith, S.H. (1994), "An exact solution of the unsteady Navier-Stokes equations resulting from a stretching surface", *ASME J. Appl. Mech.*, Vol. 61, pp. 629-33.

Soundalgekar, V.M. (1977), "Free convection effects on the Stokes problem for an infinite vertical plane", *ASME Journal of Heat Transfer*, Vol. 99, p. 499.

Stewartson, K. (1951), "On the impulsive motion of a flat plate in a viscous fluid", *Quart. Journal Appl. Math. and Mech.*, Vol. 4, p. 182.

Stokes, G.C. (1951), "On the effect of the internal friction of fluids on the motion of pendulums", *Camb. Phil. Trans.*, Vol. 8.

Wang, C.Y. (1984), "The three-dimensional flow due to a stretching flat surface", *Physics of Fluids*, Vol. 27, pp. 1915-17.